The ζ subunit of the F_1F_O-ATP synthase of α-proteobacteria controls rotation of the nanomotor with a different structure

Mariel Zarco-Zavala,* Edgar Morales-Ríos,‡ Guillermo Mendoza-Hernández,† Leticia Ramírez-Silva,† Gerardo Pérez-Hernández,§ and José J. García-Trejo*,[1]

*Departamento de Biología, Facultad de Química, and †Departamento de Bioquímica, Facultad de Medicina, Universidad Nacional Autónoma de México, Coyoacán, México; ‡Medical Research Council, Mitochondrial Research Unit, Cambridge, UK; and §Universidad Autónoma Metropolitana de México, Tlalpan, México

ABSTRACT **The ζ subunit is a novel natural inhibitor of the α-proteobacterial F_1F_O-ATPase described originally in *Paracoccus denitrificans*. To characterize the mechanism by which this subunit inhibits the F_1F_O nanomotor, the ζ subunit of *Paracoccus denitrificans* (Pd-ζ) was analyzed by the combination of kinetic, biochemical, bioinformatic, proteomic, and structural approaches. The ζ subunit causes full inhibition of the sulfite-activated PdF_1-ATPase with an apparent IC_{50} of 270 nM by a mechanism independent of the ε subunit. The inhibitory region of the ζ subunit resides in the first 14 N-terminal residues of the protein, which protrude from the 4-α-helix bundle structure of the isolated ζ subunit, as resolved by NMR. Cross-linking experiments show that the ζ subunit interacts with rotor (γ) and stator (α, β) subunits of the F_1-ATPase, indicating that the ζ subunit hinders rotation of the central stalk. In addition, a putatively regulatory nucleotide-binding site was found in the ζ subunit by isothermal titration calorimetry. Together, the data show that the ζ subunit controls the rotation of F_1F_O-ATPase by a mechanism reminiscent of, but different from, those described for mitochondrial IF_1 and bacterial ε subunits where the 4-α-helix bundle of ζ seems to work as an anchoring domain that orients the N-terminal inhibitory domain to hinder rotation of the central stalk.—Zarco-Zavala, M., Morales-Ríos, E., Mendoza-Hernández, G., Ramírez-Silva, L., Pérez-Hernández, G., García-Trejo, J. J. The ζ subunit of the F_1F_O-ATP synthase of α-proteobacteria controls rotation of the nanomotor with a different structure. *FASEB J.* 28, 2146–2157 (2014). www.fasebj.org**

Key Words: Paracoccus denitrificans · regulation

F_1F_O-ATP SYNTHASES ARE energy-transducing enzymes that produce ATP from ADP and inorganic phosphate (P_i) using the energy from electrochemical proton/sodium gradients across the plasma membrane of bacteria or the inner membranes of mitochondria and chloroplasts. Mechanistically, these enzymes consist of 2 nanomotors, coupled by rotary motion: an ion channel (F_O) and an ATP-synthesizing catalytic head (F_1). The operation of the enzyme is reversible; the direction of rotation depends on the direction of the reaction. During ATP synthesis, driven by transmembrane ion flow, rotation is clockwise (viewed from the F_O ion channel toward the F_1 catalytic head), while during ATPase-driven ion pumping, rotation is counterclockwise. To prevent the wasteful F_1-ATPase activity, the F_1F_O nanomotors of mitochondria, chloroplasts, and eubacteria are tightly controlled through mechanisms that involve various supernumerary subunits or regulatory domains (reviewed in refs. 1, 2). For instance, in mitochondria, the IF_1 inhibitor protein (3) prevents the backward F_1-ATPase activity during collapse of the proton gradient by stalling rotor gyration (4) and blocking the conformational changes of the α/β catalytic interfaces (2, 4), whereas in chloroplasts, an internal disulfide bridge of the γ subunit prevents the counterclockwise rotation in the ATPase direction (3).

Abbreviations: 1D, 1-dimensional; 2D, 2-dimensional; 2-IT, 2-iminothiolane; β-Me, β-mercaptoethanol; ΔNT, N-termainal deletion; BLAST, Basic Local Alignment Search Tool; CD, circular dichroism; DEAE, diethylaminoethyl; DEAH, diethyl aminohexyl; DSP, dithio-*bis*-succinimidylpropionate; DTT, dithiothreitol; DUF, domain of unknown function; IC_{50}, half-maximal inhibitory concentration; ITC, isothermal titration calorimetry; Js-ζ, ζ subunit of *Jannaschia* species; LDAO, lauryldimethylamine oxide; NMR, nuclear magnetic resonance; ORF, open reading frame; Pd-ε, ε subunit of *Paracoccus denitrificans*; Pd-ζ, ζ subunit of *Paracoccus denitrificans*; PdF_1, *Paracoccus denitrificans* F_1; P_i, inorganic phosphate; PK/LDH, pyruvate kinase/lactate dehydrogenase; Rs-ζ, ζ subunit of *Rhodobacter sphaeroides*; TCA, trichloroacetic acid; TEV, tobacco etch virus; SDS-PAGE, sodium dodecyl sulfate-polyacrylamide gel electrophoresis; WB, Western blot; WT, wild type

[1] Correspondence: Universidad Nacional Autónoma de México (UNAM), Facultad de Química, Departamento de Biología, Circuito Escolar, s/n, Laboratorio 206, Edificio F, Ciudad Universitaria, Coyoacán, CP 04510, México, DF. E-mail: jjgartre@unam.mx

doi: 10.1096/fj.13-241430

This article includes supplemental data. Please visit *http://www.fasebj.org* to obtain this information.

0892-6638/14/0028-2146 © FASEB

In eubacteria, the canonical inhibitor of the F_1-ATPase turnover is the ε subunit (5), which works as a ratchet to preferentially inhibit the counterclockwise rotation during ATPase turnover (6), with some evidence that it also controls the ATP synthase activity (7, 8).

In contrast to the progress toward understanding the control of the ATP synthase nanomotor in mitochondria, chloroplasts, and eubacteria, the regulatory mechanism of the F_1F_O nanomotor of α-proteobacteria was unknown until our recent isolation of the F_1-ATPase and F_1F_O-ATP synthase complexes from *Paracoccus denitrificans* (9), where we found a novel regulatory protein of 11 kDa. This subunit was named ζ, since it follows ε in decreasing size and operates as a novel strong inhibitor of the *P. denitrificans* F_1 (PdF_1)-ATPase activity. Interestingly, ζ is not related in sequence to the canonical F_1-ATPase inhibitors from eubacteria (ε) or mitochondria (IF_1). The gene encoding ζ had been identified as a hypothetical protein or domain of unknown function (DUF; DUF1476) in all α-proteobacteria (9). Moreover, a homologous ζ subunit was found associated with the ATP synthase of *Rhodobacter sphaeroides* (9), suggesting that this subunit may work as a novel inhibitor of the F_1-ATPase nanomotor all along the α-proteobacterial family.

Here we describe further functional and structural studies to resolve this novel inhibitory mechanism of the ζ subunit of the ATP synthase of *P. denitrificans*. These studies include the reconstitution of the recombinant ζ subunit into the PdF_1-ATPase, combined with cross-linking, bioinformatic, proteomic, and structural approaches. Taken together, the data resolve key features of this novel control mechanism of α-proteobacterial F_1-ATPases exerted by the ζ subunit and correlate these features with the newly resolved tertiary structure of the isolated ζ protein in solution.

MATERIALS AND METHODS

Strains

P. denitrificans (strain PD1222) was grown aerobically in the presence of succinate. Subbacterial particles (SBPs) prepared by sonication of inside-out membranes and the soluble PdF_1-ATPase were obtained as described before (9). The *Escherichia coli* strain BL21 was used to overexpress the ζ and ε subunits of *P. denitrificans* (Pd-ζ and Pd-ε, respectively) using the plasmids pIPPD1 and pEPPD1, respectively, constructed previously to clone the *P. denitrificans* ζ and ε genes (9).

Purification of PdF_1-ATPase, Pd-ζ, and Pd-ε

The PdF_1-ATPase and recombinant Pd-ε and Pd-ζ subunits were purified to homogeneity as described before (9). Additional modifications to the original purification protocol include a HiTrap Q Sepharose high-performance (QHP) column (5 ml; GE Healthcare, Little Chalfont, UK) preceding the Superdex 200 gel filtration to desalt the PdF_1-ATPase, followed by diethyl aminohexyl (DEAH) as affinity column at the final step used as reported before (9). This third chromatographic step improved the purity of the preparation (see Supplemental Fig. S1*A*). The Pd-ζ subunit was purified essentially as before (9), but the protein was eluted with a smaller KCl gradient (0–0.3 M) from diethylaminoethyl (DEAE) Sepharose followed by a Superdex 75 gel filtration step. For the purification of Pd-ε, the initial ammonium sulfate precipitation was at 15% saturation (instead of 50% as used before; ref. 9) to collect the supernatant, followed by additional 25% $(NH_4)_2SO_4$ to reach 40% saturation to precipitate the protein and resuspend the pellet containing the enriched Pd-ε. The protein was desalted by overnight dialysis against 20 mM phosphate (pH 8.0) followed by a DEAE Sepharose column, eluting the protein with a 0–0.7 M KCl gradient followed by Superdex 75, as reported before (9).

Preparation of the PdF_1-ε-ζ ($\alpha_3\beta_3\gamma\delta$) complex

Removal of the endogenous ζ and/or ε subunits from PdF_1 was carried out by immunoaffinity chromatography using protein-G agarose coupled to anti-ζ or anti-ε antibodies as described by Dunn (10). Briefly, the PdF_1-ATPase was preincubated in buffer A (250 mM sucrose, 10 mM Tris, 10% glycerol, 1 mM EDTA, 2.5 mM PAB, 0.2 mM ATP, and 30 mM sodium sulfite at pH 7.0) for 15 min before loading it into a 5 ml column of protein-G agarose coupled to anti-ζ and/or anti-ε antibodies and preequilibrated in buffer A. When the ζ was removed (without removing ε), a single protein-G-anti-ζ agarose column was used, and when both subunits were removed, 2 consecutive columns (anti-ζ and anti-ε) were coupled. Subunit composition of the eluted proteins was analyzed by sodium dodecyl sulfate-polyacrylamide gel electrophoresis (SDS-PAGE), and the fractions with reduced amounts of ζ or ε subunits relative to δ or γ (as judged from densitometry analyses) were concentrated in Centricon filters of 100 kDa cutoff. The immunoaffinity columns were washed by elution of bound ζ or ε subunits (or residual PdF_1) with 2 vol of 2 M glycine (pH 3.0) and extensive washing with PBS.

Determination of the half-maximal inhibitory concentration (IC_{50}) of the Pd-ζ in PdF_1-ATPase

The PdF_1-ATPase preparations were preincubated for 20 min at room temperature in reconstitution buffer containing 250 mM sucrose, 60 mM sodium sulfite, and 20 mM Tris (pH 8.0) with different amounts of Pd-ζ and/or Pd-ε (see **Fig. 1**). The ATPase activity was determined spectrophotometrically by the amount of P_i released from ATP as described before (9). The PdF_1-ATPase activities were obtained from the initial linear rates of P_i release (1–2 min) to avoid accumulation of the inhibitory Mg^{2+}-ADP product (9). Alternatively, in order to use another F_1-ATPase activator different to sulfite, real-time monitoring of the PdF_1-ATPase and PdF_1F_O-ATPase reactions were carried out by enzyme-coupled pyruvate kinase/lactate dehydrogenase (PK/LDH) ATPase assays as described before (11) in the presence of 0.15% lauryldimethylamine oxide (LDAO). The IC_{50} of the ζ subunit was determined by nonlinear fitting of the ATPase activity data to a Hill equation, $1 - v/V_0 = ([I]/IC_{50})^{\alpha}/[1 + ([I]/IC_{50})^{\alpha}]$, using Origin 7.5 (OriginLab Corp., Northampton, MA, USA), where V_0 is the initial catalytic rate without inhibitor, IC_{50} is the apparent inhibitor concentration that decreases the catalytic rate to $V_0/2$, and α is the Hill coefficient. The IC_{50} obtained is "apparent" since it depends on the enzyme concentration, which in this work is in the same range as that of the inhibitor; therefore, a significant fraction of the latter is bound to the enzyme (see Figs. 1 and **3**). Curve fitting with this Hill equation has been used properly before to estimate K_i values under these relatively high enzyme concentrations (12); thus, instead of an exact K_i, we estimated the apparent

IC_{50} by curve fitting with this kinetic model. It is worth noting that this Hill equation provided the best curve fitting since simpler noncompetitive kinetic models, which are valid under relatively smaller enzyme concentrations, produced fittings with higher standard errors.

Cross-linking of the PdF_1-ATPase with 2-iminothiolane (2-IT) and dithio-*bis*-succinimidylpropionate (DSP)

2-IT and DSP are dithiothreitol (DTT) or β-mercaptoethanol (β-Me) reversible and homobifunctional lysine cross-linkers of 14 and 12 Å cross-linking distance, respectively. Their reversibility is due to an internal disulfide bond suitable for resolution of cross-linked proteins by nonreducing-reducing 2-dimensional (2D)-SDS-PAGE. Cross-linking reactions were started by adding the indicated concentrations of 2-IT or DSP to the PdF_1-ATPase (diluted to 1–2 mg protein/ml) at room temperature in a buffer containing 20 mM phosphate and 10% glycerol at pH 8.0. For 2-IT cross-linking, the PdF_1-ATPase was thiolated with 1 mM 2-IT by 1 h in 20 mM phosphate buffer containing 1 mM EDTA at pH 8.0. The reaction was arrested by filtration through centrifuge Sephadex-G50 columns to remove excess cross-linker and EDTA. To oxidize neighboring thiols, 120 μM $CuCl_2$ was added and incubated for 30 min at room temperature. Afterward, thiol oxidation was arrested by removal of Cu^{2+} with 10 mM EDTA together with the addition of protease inhibitors (Complete Protease Cocktail EDTA-free; Roche, Indianapolis, IN, USA). The DSP cross-linker contains an internal disulfide; thus, a single cross-linking reaction was carried out as described before with mitochondrial F_1-ATPase (4) but without further oxidation with Cu^{2+}. The DSP cross-linking was arrested with 20 mM L-lysine after 30 min of cross-linking reaction and by filtration through centrifuge Sephadex-G50 columns. Finally, the cross-linked PdF_1-ATPase was concentrated in Amicon filters (10-kDa cutoff; Millipore, Billerica, MA, USA) and loaded into nonreducing 1D-SDS-PAGE followed by reducing 2D-SDS-PAGE, as described before (4) and detailed below. In some cases the nonreducing 1D-SDS-PAGE was transferred to a PVDF membrane and immunoblotted with antibodies anti-ε or anti-ζ as described before (9).

2D-SDS-PAGE

The cross-linked subunits of the PdF_1-ATPase were first resolved by a nonreducing 1D (12–22%) SDS-PAGE according to Laemmli (13) or Schägger and Von-Jagow (14). The lane containing the resolved cross-linked PdF_1 bands was excised and preincubated in 5% β-Me plus 10 mM DTT to reduce the disulfides formed between cross-linked proteins. Afterward, the lane was loaded horizontally on top of a 2D (16%) SDS-PAGE according to Laemmli (13) or Schägger and von Jagow (15) flanked by standard lanes. Once electrophoresis was completed, the 2D gel was subjected to Coomassie blue or Silver staining as described before (4).

Subunit ζ constructs

Construction of the N-terminal truncated (ΔNT) Pd-$\zeta^{\Delta NT}$ subunit lacking the first 14 N-terminal residues of Pd-ζ was carried out by PCR amplification of the Pd-ζ gene as described before for the cloning of the wild-type (WT) Pd-ζ^{WT} (9) using the pIPPD1 plasmid carrying the WT-ζ gene (9) to amplify the truncated Pd-$\zeta^{\Delta NT}$ with the forward oligonucleotide ζΔNTFWD 5′-TATATTGAATTCATGTTCGCCCATGATGCGG-3′ together with the original reverse primer used before (PdzCTerm) to amplify the Pd-ζ^{WT} (9). The first oligonucleotide introduced an *Eco*RI site used together with the *Hind*III site of PdzCterm for cloning of the amplified Pd-$\zeta^{\Delta NT}$ gene into pT77. The construct (pDNTPDZ1) was verified by double digest with *Eco*RI/*Hind*III and by automated sequencing showing the exact DNA sequence of the Pd-ζ^{WT} gene but lacking the first 14 residues. The designed Pd-$\zeta^{\Delta NT}$ protein starts at its N-terminal side with a Met residue before the Phe-15 of the Pd-ζ^{WT} gene. The N-terminal truncated ζ subunit of *Jannaschia* species (Js-$\zeta^{\Delta NT}$; PDB_id 2KZC) and the full Js-ζ proteins were kindly provided by Dr. Pedro Serrano and Prof. Kurt Wüthrich (Scripps Research Institute, La Jolla, CA, USA). Both Js-ζ proteins contain a His tag at the N-terminal side that was removed by tobacco etch virus (TEV) protease proteolysis before carrying out the functional PdF_1-ATPase inhibitory assays (see Supplemental Fig. S1*C*). The Js-$\zeta^{\Delta NT}$ protein lacks 19 residues from the N-terminal side of the protein and 5 residues from the C-terminal end.

Other procedures

Circular dichroism (CD) measurements were carried out using a Jasco J-715 spectropolarimeter (Jasco, Inc., Easton, MD, USA) in 0.1-cm pathlength quartz cuvettes (far-UV CD) at 25°C. The spectra shown are the average of 3 consecutive scans. Deconvolution and secondary structure calculation were carried out with the software CDNN (16). Isothermal titration calorimetry (ITC) measurements were carried out in an isothermal titration calorimeter (MicroCal model iTC200;MicroCal LLC, Northampton, MA, USA). Curve fitting to a single ATP binding site model was carried out with Origin 7.5. Protein sequences after limited proteolysis of the Pd-ζ subunit were obtained by liquid chromatography/electrospray ionization–tandem mass spectrometry (LC/ESI-MS/MS) as described before (17). Protein concentration was determined by the method of Lowry (18), modified by trichloroacetic acid (TCA) precipitation (19) as described previously (9), to avoid errors derived from interfering substances. Protein concentrations present during CD or ITC experiments were confirmed by Lowry-TCA determinations of the protein solutions recovered from the CD cuvettes or from the ITC cell after carrying out the respective determinations. Initial protein alignments were carried out by Basic Local Alignment Search Tool [BLAST; U.S. National Center for Biotechnology Information (NCBI), Bethesda, MD, USA; http://www.nlm.nih.gov/blast/] analyses and by ClustalW (http://www.clustal.org). Final alignments and phylogenetic trees were constructed with Consurf (Tel Aviv University, Tel Aviv, Israel; http://consurf.tau.ac.il/) and Chimera (University of California, San Francisco, CA, USA; http://www.cgl.ucsf.edu/chimera/).

RESULTS

Kinetic inhibitory mechanism of Pd-ζ on the PdF_1-ATPase

Previously (9), we showed that the novel 11-kDa Pd-ζ subunit found in the F_1F_O-ATP synthase of *P. denitrificans* works as a strong inhibitor of the PdF_1-ATPase activity. To estimate the IC_{50} of Pd-ζ, the recombinant ζ and ε subunits were prepared and reconstituted to the PdF_1 complex from which the endogenous ε and ζ subunits had been previously removed by immunoaffinity chromatography. Binding of the ζ subunit alone (no recombinant ε subunit present) showed a strong decay of the ATPase activity in response to increasing concentrations of Pd-ζ that was well fitted to a kinetic

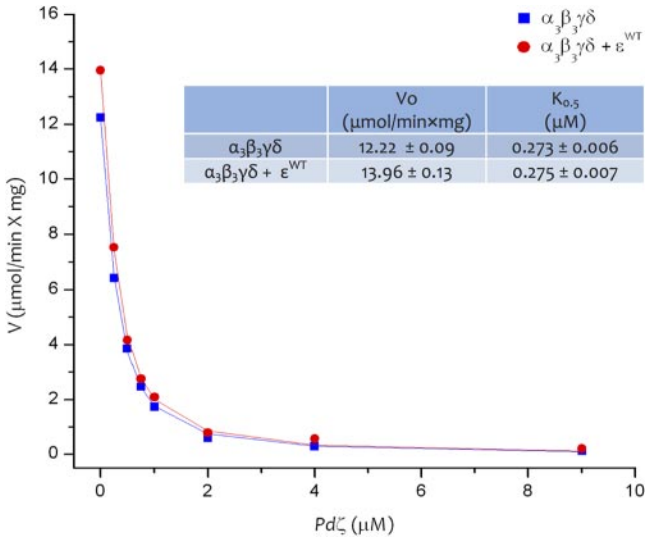

Figure 1. Inhibition of PdF_1-ATPase by increasing concentrations of the Pd-ζ subunit. PdF_1-ATPase lacking the endogenous Pd-ε and Pd-ζ ($\alpha_3\beta_3\gamma\delta$ complex; 10 μg) was preincubated for 30 min with the indicated concentrations of the isolated recombinant Pd-ζ in a total volume of 100 μl in reconstitution buffer containing 60 mM sodium sulfite before starting the ATPase reaction. Afterward, the PdF_1-ATPase-catalyzed reaction was started by addition of 10 mM of Mg^{2+}-ATP. The reaction was arrested after 2 min of reaction by adding 6% TCA, and the amount of P_i released was determined colorimetrically by the P_i release assay (see Materials and Methods). The control experiment (squares) was carried out with the $\alpha_3\beta_3\gamma\delta$ subcomplex lacking both the endogenous Pd-ε and Pd-ζ, and a parallel experiment (circles) was preceded by reconstitution of 10-fold stoichiometric excess of recombinant Pd-ε before preincubation with the indicated amounts of Pd-ζ. Trace shows the fitting to a noncompetitive kinetic model to estimate the concentration of inhibitor (Pd-ζ) necessary to achieve 50% of total inhibition. Inset: initial velocities in the absence of Pd-ζ, and estimated values of IC_{50}.

Hill model (Fig. 1 and Materials and Methods). This result confirms that Pd-ζ works as a potent total inhibitor of the PdF_1-ATPase even in conditions of maximal catalytic turnover, as exerted by sulfite. The Hill coefficient obtained with the $\alpha_3\beta_3\gamma\delta$ complex was 1.3 with or without reconstitution of ε subunit (Fig. 1), suggesting a single high-affinity site for the ζ subunit in the PdF_1-ATPase with an apparent $IC_{50} \approx 270$ nM. Furthermore, the apparent IC_{50} of Pd-ζ is essentially the same in the presence or absence of exogenous Pd-ε (Fig. 1), under conditions where exogenous ε binds efficiently to the PdF_1-ATPase (9). In summary, ε does not inhibit the PdF_1-ATPase and does not modify the affinity of exogenous Pd-ζ to inhibit the PdF_1-ATPase. It seems, therefore, that ζ substitutes ε as the inhibitory subunit in the F_1-ATPase of *P. denitrificans*. Accordingly, it is expected that removal of the ζ subunit from the PdF_1 should increase its ATPase catalytic rate. Therefore, the ζ subunit was specifically removed by anti-ζ immunoaffinity chromatography (see Materials and Methods). As expected from the observed inhibitory role of ζ, removal of ~30% of the endogenous Pd-ζ (as estimated by densitometry of Coomassie-stained SDS-PAGE) increased ~5-fold the PdF_1-ATPase turnover, from 0.88 to 4.50 $\mu mol \cdot min^{-1} \cdot mg^{-1}$ in the presence of 0.15% of LDAO. Although the latter is a less potent ATPase activator than sulfite, this result also shows that the inhibitory effect of Pd-ζ occurs irrespective of the F_1-ATPase activator used. Furthermore, removal of both subunits (ε and ζ) to obtain the $\alpha_3\beta_3\gamma\delta$ complex (see Materials and Methods) decreased to about half the sulfite-activated PdF_1-ATPase activity from 20–25 $\mu mol \cdot min^{-1} \cdot mg^{-1}$ (see Fig. 3) to 12 $\mu mol \cdot min^{-1} \cdot mg^{-1}$ (Fig. 1). Therefore, removal of ε seems to decrease the PdF_1-ATPase and therefore counteract the increase in PdF_1-ATPase activity induced by removal of ζ. In concordance with this, reconstitution of ε into PdF_1 restored partially the sulfite-activated catalytic turnover (see, for instance, the red point at 0 concentration of Pd-ζ in Fig. 1). Taken together, these data confirm that Pd-ε does not work as an intrinsic inhibitor of the PdF_1-ATPase; therefore, the ζ subunit has the key inhibitory role in the F_1-ATPase of *P. denitrificans*, and probably in related α-proteobacteria.

Evolution of the inhibitory ζ subunit of the F_1F_O-ATPase in α-proteobateria

BLAST and ClustalW alignments of the ζ subunit showed no significant similarity with bacterial (ε) or mitochondrial (IF_1) F_1-ATPase inhibitors, implying that ζ provides a novel control mechanism of the bacterial F_1F_O-nanomotor. However, alignment of the first 14 N-terminal residues of the ζ subunit with the IF_1 family showed some similarity with the inhibitory domain of the IF_1 protein (ref. 20 and Supplemental Fig. S4). It is worth noting that the ζ subunit was found as an open reading frame (ORF) or DUF1476 all along the α-proteobacterial family (**Fig. 2**) and has been found bound to the native ATP synthase of the closely related α-proteobacterium *R. sphaeroides* (9). Therefore, to determine the evolutionary relationships among homologous ζ subunits, a phylogenetic tree of the ζ subunit was constructed by the maximal likelihood method after multiple sequence alignment with 100 representative sequences of the ζ ORFs found along the α-proteobacterial family (DUF1476); from these, 12 representative protein sequences were chosen and are shown for clarity (Fig. 2*A*). In concordance with robust protein phylogenetic trees of the α-proteobaceria (21, 22), the best-scored phylogenetic tree showed that the homologous ζ subunits closest to that of *P. denitrificans* include *R. sphaeroides* and *Jannaschia* species (Fig. 2*A*). This result is in agreement with the previous observation that the ζ subunit of *R. sphaeroides* (Rs-ζ) is bound to the F_1F_O-ATP synthase of this bacterium (9). The close relationship between Pd-ζ and Js-ζ was therefore studied at the structural and functional levels as shown below. Since no ORFs or DUFs of the ζ subunit were found outside the α-proteobacterial family, the ζ subunit emerges as a regulatory subunit exclusive of the α-proteobacterial F_1F_O-ATP synthase. Furthermore, alignment of the representative ζ subunit ORFs from

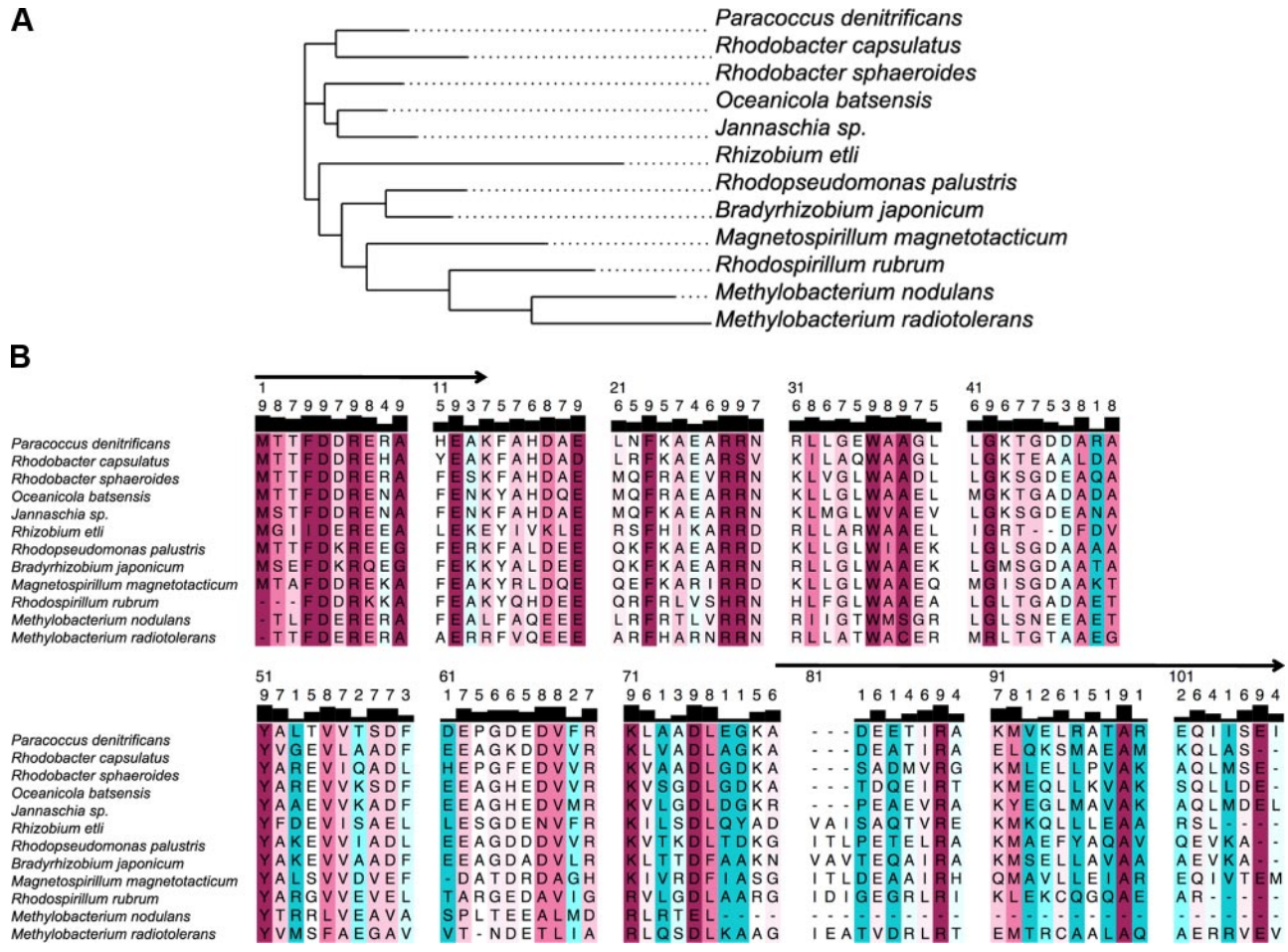

Figure 2. Evolution of the ζ subunit of the ATP synthase in α-proteobacteria. *A*) Chladrogram of the gene sequence of Pd-ζ in α-proteobacteria. ORF of the conserved Pd-ζ gene in α-proteobacteria was downloaded from BLAST. The gene appeared as a DUF in all α-proteobateria, from which 100 representative sequences were aligned with ClustalW, and a chladrogram was constructed with neighbor joining analysis, from which a small phylogenetic tree was constructed with Consurf and Chimera by maximal likelihood with 12 representative protein sequences showing the proximity of the ζ subunits of *R. sphaeroides*, *Jannaschia* species and *P. denitrificans* (PD1222). Essentially the same tree is obtained with the minimal parsimony method. *B*) Protein sequence alignment generated with Consurf with 12 ζ subunit representatives from species shown in *A* and numbered according to the Pd-ζ sequence. Amino acids are colored according to conservation, following Consurf conventions (color codes indicated: blue, variable; white, average; and cherry red, highly conserved). Conservation scores are shown in bars and numbers [scale 1 (less conserved) to 10 (totally conserved)] at top of each residue.

α-proteobacteria showed that the highly conserved residues (pink to cherry red in Fig. 2*B*) cluster on the N-terminal domain, whereas the C-terminal side has a lower density of conserved residues (blue in Fig. 2*B*), suggesting that the N-terminal side contains important functional domains, as described below.

Identification of the inhibitory domain of the ζ subunit

As a first approach to identify the inhibitory domain of the ζ subunit, the recombinant protein was subjected to limited proteolysis with trypsin, which removed 14 and 25 residues from the N- and C-terminal extremes, respectively, as found by tandem mass spectrometry analyses (Fig. 2*B*, arrows, and Materials and Methods). The purified proteolytic Pd-ζ^{15-79} fragment showed no inhibition of the PdF_1-ATPase activity at a concentration as high as 10 μM, *i.e.*, concentrations that resulted in full inhibition of the PdF_1-ATPase when the Pd-ζ^{WT} subunit was reconstituted into PdF_1 (Fig. 1). This fragment, however, binds to the enzyme since it prevented the inhibition exerted by the WT Pd-ζ when reconstituted in sub-bacterial particles. These results indicated that the inhibitory domain of the Pd-ζ subunit lies either in the first N-terminal 14 residues or in the last 25 residues near the C terminus. The proteolytic accessibility of the N and C termini indicates that both extremes of the protein are exposed and most likely highly mobile, whereas the central Pd-ζ^{15-79} domain seems resistant to the protease treatment, suggesting that it should have a rigid folded structure that competes with Pd-ζ^{WT} for binding to the PdF_1-ATPase. These features were confirmed by the Pd-ζ conformers resolved by nuclear magnetic resonance (NMR), which show a highly mobile N-terminal domain and a more rigid globular central domain (Pedro Serrano and Kurt

Wüthrich, personal communication, 2012; see Supplemental Movie S1). Although at this point the inhibitory domain of the ζ subunit could be either in the C- or N-terminal extremes, the following observations pointed to the N-terminal side of Pd-ζ as the inhibitory domain: the higher conservation of the ζ N terminus (Fig. 2*B*), the limited but significant similarity of the first 14 N-terminal residues with the inhibitory domain of IF_1 (see Supplemental Fig. S4), and the higher mobility of the N-terminal side observed in the ζ conformers (Supplemental Movie S1). Therefore, we hypothesized that the first 14 N-terminal residues of Pd-ζ contain the inhibitory domain; to assess this, these residues were removed genetically in a Pd-$\zeta^{\Delta NT}$ construct (see Materials and Methods). The recombinant Pd-$\zeta^{\Delta NT}$ construct was overexpressed in *E. coli* and purified as described for the Pd-ζ^{WT} to ~93% purity (see Materials and Methods and Supplemental Fig. S1*C*). The Pd-$\zeta^{\Delta NT}$ was reconstituted into the PdF_1-ATPase, and the inhibitory activity was measured. As shown in Fig. 3, removal of the first 14 N-terminal residues of Pd-ζ in the Pd-$\zeta^{\Delta NT}$ construct completely abolished the inhibitory capacity of the protein at concentrations as high as 9 μM, *i.e.*, concentrations that result in saturation of the Pd-ζ^{WT} and completely block PdF_1-ATPase activity (Figs. 1 and 3). These data indicate that the N-terminal side of the Pd-ζ subunit contains the inhibitory domain of the protein. To confirm that the Pd-$\zeta^{\Delta NT}$ construct keeps its native folding, a binding assay to PdF_1 was carried out by reconstitution of a 10-fold excess of Pd-$\zeta^{\Delta NT}$ (mol/mol of PdF_1) followed by gel filtration through Superdex 200. The elution profile of this reconstitution assay showed 2 elution peaks; the first consisted of the PdF_1~Pd-$\zeta^{\Delta NT}$ reconstituted complex (containing endogenous Pd-ζ and exogenously added Pd-$\zeta^{\Delta NT}$), and the second contained the free Pd-$\zeta^{\Delta NT}$ (see Supplemental Fig. S2). Furthermore, the previous reconstitution of Pd-$\zeta^{\Delta NT}$ into PdF_1 delayed the onset of inhibition exerted by the Pd-ζ^{WT} added during coupled ATPase assays, indicating that the Pd-$\zeta^{\Delta NT}$ construct binds competitively to the same binding site of the Pd-ζ^{WT} subunit of the PdF_1-ATPase. Remarkably, these results show that the Pd-$\zeta^{\Delta NT}$ construct keeps its native folded structure that binds to the PdF_1-ATPase and suggest that the globular domain of Pd-ζ works as an anchoring domain of this inhibitory protein, whereas the N terminus harbors the inhibitory domain of the protein.

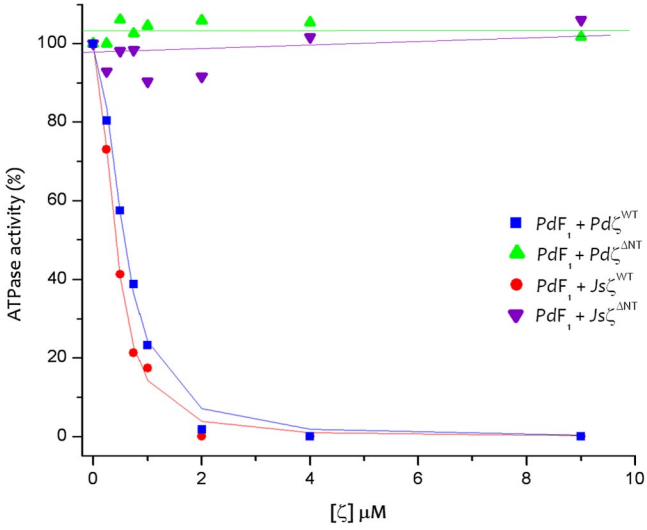

Figure 3. N-terminal domain of the Pd-ζ subunit is the inhibitory region of the protein, and this inhibitory function is conserved in Js-ζ. PdF_1-ATPase (10 μg) was preincubated for 30 min with the indicated concentrations of the recombinant Pd-ζ^{WT}, Pd-$\zeta^{\Delta NT}$, Js-ζ^{WT}, and Js-$\zeta^{\Delta NT}$ proteins in a total volume of 90 μl in reconstitution buffer before starting the ATPase reaction. Afterward, the PdF_1-ATPase-catalyzed reaction was started by adding 10 μl of Mg^{2+}-ATP to the premixed PdF_1 and the respective ζ subunits to obtain a final concentration of 10 mM Mg^{2+}-ATP in a reaction mixture containing 60 mM sodium sulfite (see Materials and Methods). The reaction was arrested after 1 min of reaction by adding 6% TCA, and the amount of P_i released was determined colorimetrically by the P_i assay (see Materials and Methods). Trace shows the fitting to a Hill kinetic model. Maximum (100%) control activity corresponded to 17–20 $\mu mol \cdot min^{-1} \cdot mg^{-1}$ for Js-$\zeta^{\Delta NT}$, Js-ζ^{WT}Pd-ζ^{WT}, and Pd-$\zeta^{\Delta NT}$ titration curves with IC_{50} values of 0.57 ± 0.03 μM for Pd-ζ^{WT} and 0.41 ± 0.02 μM for Js-ζ^{WT}. Data points are averages of 3 independent experiments for each curve and had an SD of 10% (omitted for clarity).

Conservation of the inhibitory function of the ζ subunit in the α-proteobacterial family

To confirm the inhibitory role of the ζ subunit in other α-proteobacteria, we looked to isolate the homologous ζ subunit from another member of this bacterial class. Coincidentally, the NMR structure of a homologous ζ protein was reported in the NCBI BLAST server (PDB_id 2KZC). This protein was a member of the DUF1476 family in *Jannaschia* species, another α-proteobacterium closely related to *P. denitrificans* (Fig. 2). This structure was uploaded by the group of Kurt Wüthrich, who kindly provided the full Js-ζ subunit. The Js-ζ subunit was reconstituted into the PdF_1-ATPase in the same conditions used for the Pd-ζ^{WT} (Fig. 1). As shown in Fig. 3, the Js-ζ protein also worked as a strong inhibitor of the PdF_1-ATPase, with apparent IC_{50} (0.41 μM) and Hill coefficient ($\alpha=2$) very similar to those of the Pd-ζ^{WT} (0.57 μM and $\alpha=2$). These IC_{50} and α values obtained with the whole PdF_1-ATPase (Fig. 3) are higher than those obtained with the PdF_1-ε-ζ (Fig. 1), most likely because in the $\alpha_3\beta_3\gamma\delta$ complex, the exogenous recombinant ζ binds more efficiently in the absence of the endogenous ζ and ε than in the PdF_1-ATPase. Most important, the titration curve of Js-ζ *vs.* PdF_1-ATPase activity superimposed with that of Pd-ζ (Fig. 3), reflecting the high similarity (85.6%) and identity (58.6%) between Js-ζ and Pd-ζ (see Supplemental Fig. S5). Although further studies with other α-proteobacteria more distant to *P. denitrificans* are ongoing to reinforce this conclusion, these results strongly suggest that the ζ subunit works as a potent F_1F_O-ATPase inhibitor all along the α-proteobacteria class.

In addition to the PdF_1-ATPase inhibition by the

complete Js-ζ, functional reconstitution studies were also carried out with the truncated Js-$\zeta^{\Delta NT}$ protein originally resolved by NMR (PDB_id 2KZC), which lacks the first N-terminal 19 residues (and the last 5 C-terminal ones). As expected from the lack of inhibitory function of the Pd-$\zeta^{\Delta NT}$ construct (Fig. 3), this truncated protein was also unable to inhibit the PdF_1-ATPase activity (Fig. 3). Furthermore, since the Js-$\zeta^{\Delta NT}$ subunit folds nearly identically with a 4-α-helix bundle as the WT Pd-ζ (P. Serrano and K. Wüthrich, personal communication, 2012; see PDB_id 2KZC), it can be inferred that the removal of 19 N-terminal residues from Js-ζ (or the 14 N-terminal residues from Pd-ζ) does not affect its overall folding, since the central 4-α-helix bundle remains properly folded. In summary, the loss of inhibitory PdF_1-ATPase function of the Pd-$\zeta^{\Delta NT}$ and the Js-$\zeta^{\Delta NT}$ truncated proteins does not result from defective folding but from the removal of their respective inhibitory N-terminal domains. This conclusion is better ascertained from the Pd-$\zeta^{\Delta NT}$ construct, since it lacks the first 14 N-terminal residues, whereas the Js-$\zeta^{\Delta NT}$ construct lacks 19 residues from N terminus and also 5 residues from the C-terminal side.

Structure of the isolated ζ subunit of α-proteobacterial ATP synthase

To understand the structure-function relationships inherent to this novel control mechanism of the α-proteobacterial F_1-ATPase, the secondary structure of the isolated ζ subunit was first analyzed by CD. These analyses showed that the Pd-ζ^{WT} subunit is an all-α-helix protein with an α-helix content $>$ 90% at pH 6.0 and pH 8.0 (Supplemental Fig. S6). Subsequently, in collaboration with Kurt Wüthrich, the NMR structure of the recombinant Pd-ζ was resolved. The structure (PDB_id 2LL0) was part of a preliminary report (23) that will be described in detail elsewhere (P. Serrano and K. Wüthrich, personal communication, 2012). The NMR structure of the isolated Pd-ζ exhibits a novel 4-α-helix bundle tertiary structure, different from that of the known F_1-ATPase inhibitors, *i.e.*, bacterial ε and mitochondrial IF_1, which are α + β and extended α-helix proteins, respectively (see **Fig. 6**). The N and C termini of ζ converge in the tertiary structure of the protein, where the N-terminal side protrudes from the globular 4-α-helix central domain (see Fig. 6*B*). The NMR structure of Pd-ζ was resolved at pH 6.0 and not at pH 8.0 (the optimal inhibitory pH of Pd-ζ) to avoid the extensive proton exchange with the solvent, which hinders the resolution of several NMR peaks. To confirm that the secondary structure of Pd-ζ is preserved at pH 6.0, CD spectra of Pd-ζ were obtained at both pH values, resulting in ellipticity traces that superimposed almost identically (Supplemental Fig. S6), indicating a similar secondary structure of the Pd-ζ subunit at both pH values.

Cross-linking of Pd-ζ with neighboring subunits of the rotor and the stator of the PdF_1-ATPase

To determine the locus of the ζ subunit in the quaternary structure of the PdF_1-ATPase, the endogenous Pd-ζ subunit was cross-linked with neighboring subunits in the PdF_1-ATPase with 2-IT. This cross-linker produced Pd-ζ adducts of ~26, 41, and 65–70 kDa (**Fig. 4**). The sizes of these adducts suggested the following cross-linking products: ζ-ε (11+16=27 kDa), ζ-γ (11+30=41 kDa), ζ-α (11+50=61 kDa), and ζ-β (11+55=66 kDa) (Fig. 4*A*, right panel). To confirm the identity of

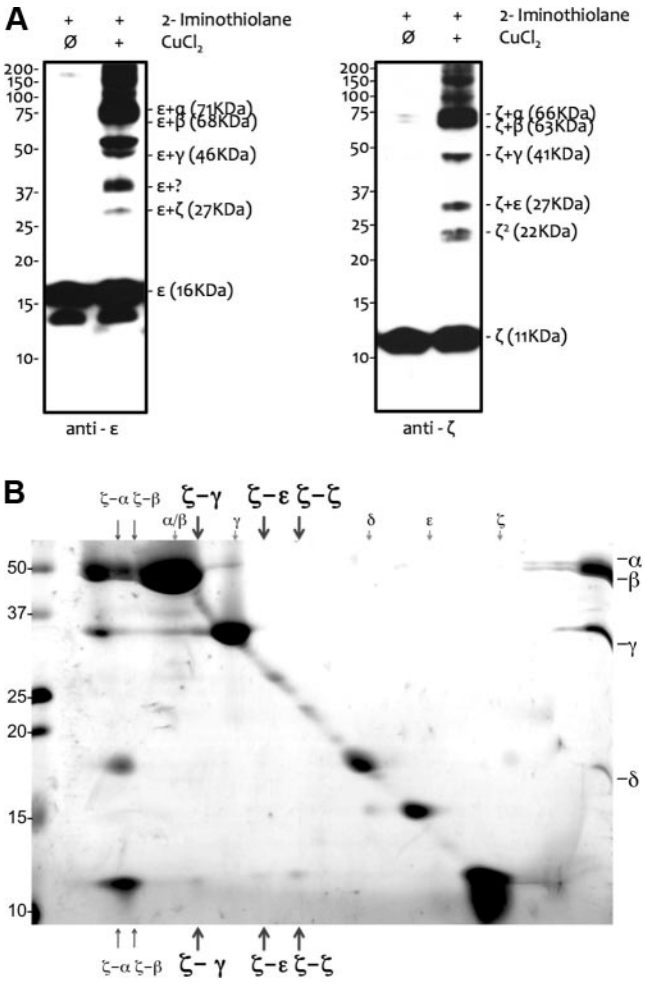

Figure 4. Reversible cross-linking of Pd-ζ and Pd-ε with rotor and stator subunits of the PdF_1-ATPase. *A*) Top: 20 μg of the PdF_1-ATPase containing its endogenous Pd-ε and Pd-ζ were thiolated on accessible lysine residues with 1 mM 2-IT; afterward, reversible disulfide cross-linking was induced by incubation with 120 μM $CuCl_2$ where indicated. WB anti-ε (left) and anti-ζ (right) of control (first lanes) and cross-linked enzymes (right lanes) were carried out as described in Materials and Methods. Major cross-linking products obtained were ε-α, ε-β, ε-γ, ζ-α, ζ-β, and ζ-γ adducts. Smaller products included a low-yield ε-ζ adduct. *B*) Identities of these adducts are confirmed as follows: 900 μg of PdF_1-ATPase cross-linked with 1 mM 2-IT as in *A* were overloaded on a nonreducing 1D-SDS-PAGE according to Laemmli (13). Afterward, the entire lane containing the cross-linked PdF_1-ATPase was reduced with 5% β-Me and 10 mM DTT for 0.5 h before loading it into a 2D-SDS-PAGE according to Schagger and Von Jagow (14). Smaller spots aligned vertically under the major spots aligned diagonally (arrows) indicate cross-linked subunits, which are identified with the right (PdF_1-ATPase) and left (MWS) standard lanes. Major cross-linking products resolved are ζ-α, ζ-β, and ζ-γ as observed in *A*. Positions of ζ-ε and ζ-ζ cross-linking adducts are also indicated.

these cross-linking products, Western blot (WB) analyses with anti-ζ and anti-ε antibodies were carried out. The 27-kDa adduct had cross-reactivity with both antibodies (Fig. 4*A*), thus confirming the cross-linking between ζ and ε. The putative ζ-γ adduct of ~41 kDa and other cross-linking products were resolved as vertically aligned spots in a reducing 2D-SDS-PAGE. The final 2D gel showed clearly all the Pd-ζ cross-linking products previously observed by WB (compare Fig. 4*A*, *B*). The observed ζ cross-linking subunits are (Fig. 4*B*, left to right) ζ-α, ζ-β, and ζ-γ (Fig. 4*B*, dark arrows); a low yield ζ-ε; and a ζ-ζ cross-linking that may result from dimeric Pd-ζ, as observed before with mitochondrial IF_1 (4). The presence of a ζ-ζ dimer is also suggested by gel filtration of the isolated Pd-ζ, which eluted as 2 peaks from Superdex 75. To discard the possibility that the observed Pd-ζ cross-linkings resulted from nonspecific thiol oxidation by Cu^{2+}, similar cross-linking experiments were carried out with DSP, a similar cross-linker that already contains an internal disulfide, and therefore thiol oxidation with Cu^{2+} was not necessary. Cross-linking with DSP showed ζ-γ (11+30=41 kDa), ζ-α (11+50=61 kDa), and ζ-β (11+55=66 kDa) adducts (see Supplemental Fig. S2) similar to those observed with 2-IT (Fig. 4*A*), with the exception of ζ-ε and ζ-ζ. These results show that the observed ζ-cross-linkings (ζ-α, ζ-β, and ζ-γ) do not result from nonspecific thiol oxidation but from actual cross-liking interactions between the latter PdF_1 subunits. Furthermore, the relatively low ζ-γ cross-linking yields obtained with 2-IT and DSP (Fig. 4 and Supplemental Fig. S2) were increased by previous reconstitution of excess ζ subunit into PdF_1 followed by gel filtration through Superdex 200 to remove the free recombinant subunit before cross-linking. In sum, the cross-linking data show that the ζ subunit interacts with rotor (γ) and stator (α, β) subunits of the PdF_1-ATPase, strongly suggesting that the ζ subunit interferes with rotation of the central rotor, a result reminiscent of those observed with mitochondrial IF_1 and bacterial ε as derived from cross-linking (4, 6) and crystallographic studies (24–28).

Nucleotide binding to the ζ subunit of *P. denitrificans*

The eubacterial ε subunit binds ATP (29), and it was of interest to examine whether this is also the case for Pd-ζ. The first evidence of nucleotide binding to Pd-ζ was obtained by NMR experiments of Pd-ζ carried out in the presence of ATP or ADP (P. Serrano and K. Wüthrich, personal communication, 2013). Therefore, we estimated the binding affinity of ATP to Pd-ζ by ITC. The isothermal titration of ATP into the isolated ζ subunit was fitted to a single binding site with a K_d of 11.4 mM (**Fig. 5**). Similar calorimetric experiments also showed the binding of ADP to Pd-ζ but with a lower affinity (not determined). Given the low affinity of the nucleotide binding site observed, the protein concentration of ζ was relatively high (60 mg/ml), and to avoid excessive heat of dilution of the protein, the nucleotide

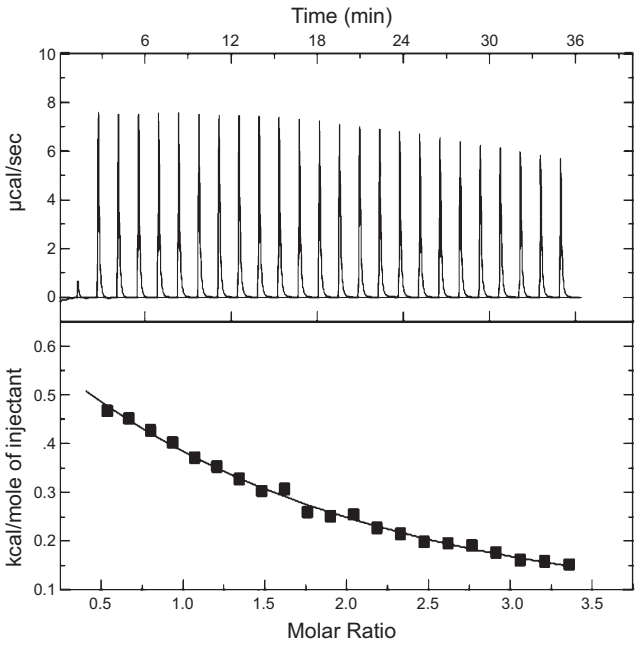

Figure 5. Calorimetric isothermic titration of ATP binding to Pd-ζ. Pd-ζ subunit was preequilibrated at 25°C at a concentration of 60 mg/ml in reconstitution buffer (see Materials and Methods). Once the system was stabilized, the calorimeter cell was automatically titrated with the indicated injections from an ATP stock solution of 82.14 mM in the injection syringe. Heat peaks of the injections were integrated manually to avoid errors in automatic peak detection, and dilution heat of the ATP stock was subtracted from a parallel experiment with the same injection program but in the absence of Pd-ζ in the calorimeter cell. After dilution heat of the nucleotide was subtracted, heat of ATP binding was fitted to a nonlinear single binding site, as shown by black trace. Dissociation constant obtained was 11.4 mM.

was injected into the cell containing the protein, and the heat of dilution of the nucleotide (determined with control injections without the protein in the cell) was subtracted from the trace containing the ζ subunit to obtain a good curve fitting (Fig. 5). To confirm the binding of nucleotides into the isolated Pd-ζ subunits, the structure of the Pd-ζ protein was resolved by NMR in the presence of ADP (P. Serrano and K. Wüthrich, personal communication, 2013), and the resulting structure (PDB_id 2MDZ) was different from that of the isolated Pd-ζ (PDB_id 2LL0). Although the detailed differences between the isolated *apo*Pd-ζ and the ADP-bound Pd-ζ structures will be presented in detail elsewhere (P. Serrano and K. Wüthrich, personal communication, 2013), the overall results confirm the existence of a low-affinity nucleotide binding site in the Pd-ζ subunit.

DISCUSSION

Kinetic inhibitory mechanism of Pd-ζ on the PdF_1-ATPase

Previously, we found that the ζ subunit was a potent inhibitor of the PdF_1-ATP synthase (9); however, the

putative participation of the ε subunit in this inhibitory mechanism remained to be clarified. Here, by working with an $\alpha_3\beta_3\gamma\delta$ complex lacking the endogenous ε and ζ subunits (PdF_1-ζ-ε), it was possible to assess the functional effects of recombinant ε and ζ by separate or joint reconstitution of both subunits into the PdF_1-ζ-ε complex. As expected from the inhibitory role of ζ, removal of this subunit increased severalfold the steady-state PdF_1-ATPase activity. Furthermore, the PdF_1-ζ-ε ATPase activity decreased to 0 in response to increasing ζ concentrations, with a decay well fitted to a Hill equation and $\alpha = 1.3$, suggesting a single inhibitory binding site with apparent $IC_{50} \approx 0.27$ mM. Furthermore, when the ζ subunit was reconstituted into the PdF_1-ATPase containing the endogenous ε and ζ subunits, the Hill coefficient raised from $\alpha = 1.3$ in the $\alpha_3\beta_3\gamma\delta$ complex to $\alpha = 2$, and the apparent IC_{50} increased ~2-fold (compare Figs. 1 and 3, respectively). Although these results might suggest a ζ/PdF_1 stoichiometry >1, it is possible that the presence of the endogenous ζ and ε subunits in the PdF_1 have raised the α and apparent IC_{50} values. Thus, although further reconstitution and binding assays are necessary (and in course) to determine more accurately the ζ/PdF_1 stoichiometry and K_i values, the present data suggest that the ζ subunit binds to a single binding site of high affinity to exert full inhibition the PdF_1-ATPase. By comparison, the K_i values of eubacterial ε (≈10 nM; ref. 5) and mitochondrial IF_1 (≈0.4 μM; refs. 30, 31) were determined under similar relatively high enzyme concentrations; thus, the apparent IC_{50} of PdF_1 for the ζ subunit of ≈0.27 μM resulted in the same range. Remarkably, the ε subunit did not exert inhibition of the PdF_1-ATPase either directly or indirectly, *i.e.*, as a factor promoting the binding of the ζ subunit (Fig. 1). Furthermore, removal of ε decreased the PdF_1-ATPase activity, and the latter improved partially after ε reconstitution (Fig. 1). Since ε has been described as the canonical inhibitor of bacterial F_1-ATPases, it is of relevance to find here that this subunit does not work as such intrinsic inhibitor in *P. denitrificans*, suggesting that the ζ subunit substitutes ε as the natural F_1-ATPase inhibitor in the whole α-proteobacteria class. Similar to the noninhibitory properties of Pd-ε, the homologous subunit of *Bacillus subtilis* was recently described as F_1-ATPase activator rather than inhibitor, acting by relieving the intrinsic inactivation of the enzyme exerted by endogenous Mg^{2+}-ADP (32). Thus, the lack of inhibitory function of the ε may not be exclusive of α-proteobacteria but this may be extended to gram-positive bacteria.

Conservation of the primary sequence and inhibitory function of the ζ subunit in the α-proteobacterial family

According to the endosymbiotic theory (33) and robust phylogenetic analyses (21, 22), *P. denitrificans* and other α-proteobacteria are closely related to the protoendosymbiont from which mitochondria emerged. This suggested that ζ could be an evolutive predecessor of mitochondrial IF_1. However, the overall sequence of ζ does not align with mitochondrial IF_1 or ε subunits, suggesting that the limited similarity of its N-terminal inhibitory domain with that of IF_1 (Supplemental Fig. S4) is a case of structural evolutive convergence. This N-terminal inhibitory domain of ζ is highly conserved along α-proteobacteria (Fig. 2), whereas its C-terminal side is rather variable, indicating the functional relevance of the N-terminal domain. Coincidentally, some of the ζ homologues closer to that of *P. denitrificans* were found in *R. sphaeroides* and *Jannaschia* species (Fig. 2). Accordingly, given the similarity between Pd-ζ and Rs-ζ, it was possible to immunodetect the homologous ζ subunit of *R. sphaeroides* as an integral ATP synthase subunit (9). However, the putative inhibitory function of other ζ subunits homologous to that of *P. dentitrificans* remained to be demonstrated. Therefore, the observation that the ζ subunit from *Jannaschia* species worked as a strong inhibitor of the Pd-F_1 ATPase with a similar IC_{50} compared with that of Pd-ζ (Fig. 3) confirmed that the inhibitory function of the ζ subunit is conserved in other α-proteobacteria. On the other hand, the central globular and C-terminal portions of the ζ subunit are different in primary and tertiary structure to mitochondrial IF_1 and bacterial ε, and consequently, some of their functional properties differ as well. For instance, the conserved regulatory histidine pairs (34, 35) of IF_1 that enhance F_1-ATPase inhibition at pH <7 are absent in the ζ subunit and consequently, the optimal pH of Pd-ζ is different (~pH 8). On the other hand, the ATP binding motif of ε [I(L)DXXRA; ref. 36] is absent in the ζ subunit although the latter binds ATP with relatively low affinity (Fig. 5); thus, the ζ subunit possesses a new ATP binding motif that remains to be defined. In summary, the data show that the ζ subunit is highly conserved along α-proteobacteria as a novel F_1-ATPase inhibitor and differs in primary and tertiary structure to the canonical ε and IF_1 inhibitors of eubacteria and mitochondria, respectively.

N-terminal inhibitory domain, cross-linking, and structure of the ζ subunit

As predicted from domain conservation (Fig. 2) and limited proteolysis of ζ, the Pd-$\zeta^{\Delta NT}$ construct is unable to inhibit the rotary PdF_1-ATPase turnover (Fig. 3), although it preserves its 4-α-helix globular structure (PDB_id 2KZC) and it binds to the PdF_1 (Supplemental Fig S2). These results show that the first 14 N-terminal residues of the ζ subunit harbor the inhibitory domain of the protein. Together with the ζ-γ cross linking observed (Fig. 4), the data suggest that the ζ subunit inserts its highly mobile inhibitory N-terminal domain in an $\alpha/\beta/\gamma$ interface to block γ/ε rotation and/or the α/β catalytic movements of the PdF_1-ATPase (Fig. 5 and Supplemental Movie S1). This is reminiscent of the inhibitory mechanisms of bacterial ε and mitochondrial IF_1 to block rotation of their respective F_1-ATPases (24, 26–28). However, the ζ subunit shows functional simi-

larities but structural differences with these well-known F_1-ATPase inhibitors. For instance, the ζ subunit shows hybrid properties of ε (such as ATP binding) and IF_1 (such as an N-terminal inhibitory domain) but possesses a remarkably different structure (**Fig. 6**). Furthermore, the N-terminal domain of ζ is highly mobile (Supplemental Movie S1), and it does not acquire a full α-helical conformation (Fig. 6*B*), as compared with the inhibitory α-helical domains of ε and IF_1 bound to their respective F_1-ATPases (24, 26–28). Furthermore, ε and IF_1 have different interactions with rotor and stator interfaces to block rotation of mitochondrial and bacterial F_1-ATPases (24, 26–28). Whereas ε is a rotary subunit that works as a ratchet and contacts mainly the γ subunit, mitochondrial IF_1 is part of the stator and shows more contacts with an α/β interface than with the rotary γ subunit (24, 26–28). This suggests that the ζ subunit blocks rotation of the PdF_1-ATPase by interacting with an α/β/γ interface but with rotor/stator interactions that may be different from those observed for ε and IF_1 (24, 26–28). On the other hand, regarding the central 4-α-helical globular domain of the ζ subunit, the observation that the Pd-$\zeta^{\Delta NT}$ construct is able to bind to the PdF_1-ATPase (Supplemental Fig. S2) without exerting F_1-ATPase inhibition (Fig. 3) suggests that this portion of the protein works as an anchoring domain of ζ, preserving its 4-α-helix structure after binding to the PdF_1-ATPase. The higher cross-linking yields of the ζ-α and ζ-β adducts compared with ζ-γ and ζ-ε (Fig. 4) suggest that the anchoring domain of ζ is part of the stator and that the N terminus of this inhibitor sticks to the rotary γ subunit to block rotation.

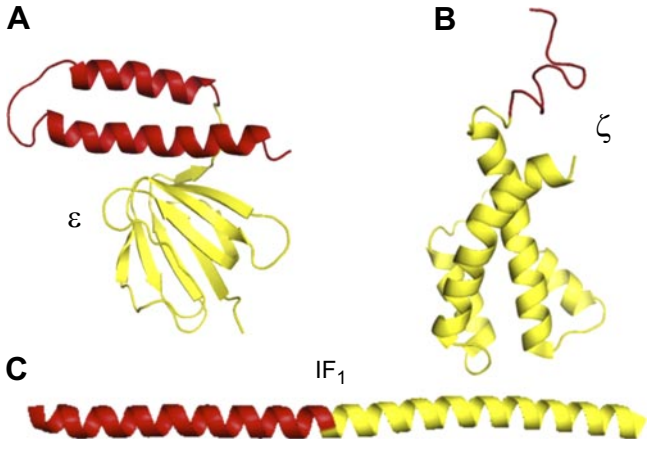

Figure 6. Structures of the F_1-ATPase protein inhibitors and their inhibitory domains. *A*) X-ray structure of the ε subunit for *E. coli* (Ec-ε; PDB_id 1AQT). *B*) X-ray structure of the inhibitor protein IF_1 from *Bos taurus* (PDB_id 1HF9). *C*) NMR solution structure of the ζ inhibitory protein from *P. denitrificans* (PDB_id 2LL0). In all structures, the segment in red shows the inhibitory domains, which correspond to the C-terminal 2-α-helixes of Ec-ε (*A*), the mobile N-terminal 14 residues of Pd-ζ (*B*), and the N-terminal IF_1 region of mitochondrial F_1-ATPase. The cross-linking (Fig. 4) and structural comparison indicates that the inhibitory domain of Pd-ζ sticks into a rotor/stator interface to block rotary catalysis of the PdF_1-ATPase (see text for details).

Accordingly, the N terminus of ζ contains only 2 Lys residues (Fig. 2*B*) that likely produce a low ζ-γ cross-linking yield (Fig. 4), whereas the globular anchoring domain of ζ possesses 4 Lys residues, likely forming ζ-α/ζ-β adducts of higher cross-linking yields compared with ζ-γ (Fig. 4). However, the structural details of the inhibitory conformation of ζ bound to the PdF_1-ATPase are yet to come after ongoing structural studies at atomic resolution.

Nucleotide binding site of the ζ subunit

Finding a low-affinity nucleotide binding site on the ζ subunit (Fig. 6) suggests that the inhibitory function of this protein may be regulated by ATP or ADP binding, as found with eubacterial ε subunit. Comparing the low-affinity nucleotide binding site of ζ with that of eubacterial ε, it is worth mentioning that the *E. coli* ε subunit binds ATP with a K_d of 22 mM (36), whereas that of thermophilic bacterium PS3 binds it with a K_d of 200 μM (37). ATP binding to ε seems to control the inhibitory/noninhibitory transitions of ε (25, 29). Furthermore, some functional antecedents of the ATP synthase of *P. denitrificans* also indicate the regulatory effects of ATP or ADP. For instance, it has been shown that the continuous PdF_1F_O-ATPase activity of membrane vesicles from *P. denitrificans* requires the presence of ADP in the medium (38, 39), and that the forward PdF_1F_O-ATP synthase activity is inhibited by product ATP (40, 41). However, the apparent binding affinities for ADP and ATP that control the PdF_1F_O-ATPase/ATP synthase turnover are in the micromolar range (38–41), *i.e.*, affinities $\sim 10^3$ times higher than the low-affinity K_d observed for ATP with the isolated ζ subunit (Fig. 5). Thus, further functional studies are required to assess the putative regulatory role of the ATP/ADP binding site of the ζ subunit on the functional PdF_1 and F_1F_O-ATPase complexes.

CONCLUSIONS

In summary, several key features of the new inhibitory ζ subunit of the α-proteobacterial F_1-ATPase were here resolved and are enlisted as follows. The strong inhibition of PdF_1 exerted by the ζ subunit appears to require 1 mol/mol of enzyme, and its binding is independent of the ε subunit of α-protobacteria, which is not by itself an inhibitor. The ζ subunit is a natural F_1-ATPase inhibitor conserved all along the α-proteobacteria class. The highly conserved and protruding N-terminal domain of the ζ subunit is the inhibitory domain of the protein, whereas the globular 4-α-helix part of the protein seems to work as an anchoring domain. The structure of the ζ subunit is essentially different from the other known F_1-ATPase inhibitors, IF_1 and ε. Cross-linking studies place the ζ subunit at a rotor (γ)/stator (α, β) interface, which indicates that the inhibitory mechanism of the ζ subunit involves the interference with rotation of the central stalk. The subunit has a nucleotide binding site whose function

remains to be evaluated. In sum, from the functional and structural differences observed between the ζ subunit and the ε or IF_1 canonical F_1-ATPase inhibitors, this work provides the basis of a new control mechanism of the bacterial F_1F_O-ATP synthase nanomotor, particularly conserved in α-proteobacteria. FJ

The authors gratefully acknowledge Marietta Tuena de Gómez-Puyou and Armando Gómez–Puyou [Institute of Cell Physiology (IFC), Universidad Nacional Autónoma de México (UNAM)] for critical review of this work. The authors also thank John E. Walker (Medical Research Council, Mitochondrial Biology Unit, Cambridge, UK) for important suggestions in the first draft of the article. The authors also thank Blanca Barquera (Rensselaer Polytechnic Institute, Troy, NY, USA) and Roderick A. Capaldi (University of Oregon, Eugene, OR, USA) for important suggestions to improve the final text of this article. The technical assistance of Raquel Ortega is gratefully acknowledged. This project was supported by the following grants to J.J.G.-T.: Programa de Apoyo a Proyectos de Investigación e Innovación Tecnológica (PAPIIT)–Dirección General Asuntos del Personal Académico (DGAPA; UNAM) grants IN213809 and IN211012, and Consejo Nacional de Ciencia y Tecnología (CONACyT) grant CB-2011-01-167622. G.P.-H. was supported by CONACyT grants 47310013 and 105532 and L.R-S. by PAPIIT-DGAPA (UNAM) grant IN215912. The authors are grateful to Dr. Pedro Serrano and Prof. Kurt Wüthrich for initial collaborative work in the resolution of the NMR structure of the Pd-ζ subunit, for permission to show the resolved Pd-ζ structure (PDB_id 2LL0; Fig. 6 and Supplemental Movie S1) and to cite the nucleotide binding properties of the ζ subunit, and for providing plasmids expressing the truncated and full Js-ζ subunits for functional studies (Pedro Serrano, M. G. Biswaranjan Mohanty, and Kurt Wüthrich; to be submitted; private communication by the authors). M.Z.-Z. was supported by CONACyT Ph.D. Fellowship 299475; this work is part of her Ph.D. thesis at the Postgraduate Studies in Biomedical Sciences of UNAM [Doctorado en Ciencias Biomédicas (PDCB)] carried out at the UNAM Facultad de Química (Faculty of Chemistry) with J.J.G.-T. as Ph.D. advisor. Author contributions: M.Z.-Z. carried out most of the experiments, including protein purification, cross-linking, CD, calorimetry, limited proteolysis, ATPase activity, WB, and 2D-SDS-PAGE gels, designed research, made gene constructions, and analyzed the data; E.M.R. carried out preliminary biochemical experiments shown in Supplemental Material, designed the primers for protein constructions and carried out the phylogenetic analysis of the ζ gene in the α-proteobacterial class, wrote part of Materials and Methods, and contributed key expertise in the cloning and protein purification protocols; G.M.-H. carried out the mass spectrometry sequencing of the full WT Pd-ζ subunit and also protein constructs and proteolytic fragments obtained by limited proteolysis; L.R-S. carried out the CD experiments and helped with the calculation of secondary structure content of the Pd-ζ subunit; G.P.-H. carried out ITC of ATP binding to Pd-ζ and helped with the data fitting to estimate the K_d for ATP; J.J.G.-T. designed research, carried out cross-linking experiments, ATPase assays, and protein purification experiments and contributed to molecular biology constructions and cloning, helped with curve fitting to estimate the IC_{50} of Pd-ζ during inhibitory titration, carried out 2D-SDS-PAGE gels, constructed phylogenetic trees and protein sequence alignments, and wrote the manuscript. The authors declare no conflicts of interest.

Dedication: This work is dedicated to the memory of Armando Gómez-Puyou, emeritus professor of the Universidad Nacional Autónoma de México (UNAM), for his major contributions to bioenergetics and protein structure and function, and as one of the most important scientists of Mexico, and also to Guillermo Mendoza-Hernández for his major contributions to proteomics at UNAM.

REFERENCES

1. Garcia-Trejo, J. J., and Morales-Rios, E. (2008) Regulation of the F1F0-ATP synthase rotary nanomotor in its monomeric-bacterial and dimeric-mitochondrial forms. *J. Biol. Phys.* **34,** 197–212
2. Walker, J. E. (2013) The ATP synthase: the understood, the uncertain and the unknown. *Biochem. Soc. Trans.* **41,** 1–16
3. Pullman, M. E., and Monroy, G. C. (1963) A naturally occurring inhibitor of mitochondrial adenosine triphosphatase. *J. Biol. Chem.* **238,** 3762–3769
4. Minauro-Sanmiguel, F., Bravo, C., and Garcia, J. J. (2002) Cross-linking of the endogenous inhibitor protein (IF1) with rotor (gamma, epsilon) and stator (alpha) subunits of the mitochondrial ATP synthase. *J. Bioenerg. Biomembr.* **34,** 433–443
5. Sternweis, P. C., and Smith, J. B. (1980) Characterization of the inhibitory (epsilon) subunit of the proton-translocating adenosine triphosphatase from *Escherichia coli*. *Biochemistry* **19,** 526–531
6. Tsunoda, S. P., Rodgers, A. J., Aggeler, R., Wilce, M. C., Yoshida, M., and Capaldi, R. A. (2001) Large conformational changes of the epsilon subunit in the bacterial F1F0 ATP synthase provide a ratchet action to regulate this rotary motor enzyme. *Proc. Natl. Acad. Sci. U. S. A.* **98,** 6560–6564
7. Masaike, T., Suzuki, T., Tsunoda, S. P., Konno, H., and Yoshida, M. (2006) Probing conformations of the beta subunit of F0F1-ATP synthase in catalysis. *Biochem. Biophys. Res. Commun.* **342,** 800–807
8. Iino, R., Hasegawa, R., Tabata, K. V., and Noji, H. (2009) Mechanism of inhibition by C-terminal alpha-helices of the epsilon subunit of *Escherichia coli* FoF1-ATP synthase. *J. Biol. Chem.* **284,** 17457–17464
9. Morales-Rios, E., de la Rosa-Morales, F., Mendoza-Hernandez, G., Rodriguez-Zavala, J. S., Celis, H., Zarco-Zavala, M., and Garcia-Trejo, J. J. (2010) A novel 11-kDa inhibitory subunit in the F1FO ATP synthase of *Paracoccus denitrificans* and related alpha-proteobacteria. *FASEB J.* **24,** 599–608
10. Dunn, S. D. (1986) Removal of the epsilon subunit from *Escherichia coli* F1-ATPase using monoclonal anti-epsilon antibody affinity chromatography. *Anal. Biochem.* **159,** 35–42
11. Garcia, J. J., Tuena de Gomez-Puyou, M., and Gomez-Puyou, A. (1995) Inhibition by trifluoperazine of ATP synthesis and hydrolysis by particulate and soluble mitochondrial F1: competition with H2PO4. *J. Bioenerg. Biomembr.* **27,** 127–136
12. Halfman, C. J., and Marcus, F. (1982) A method for determining kinetic parameters at high enzyme concentrations. *Biochem. J.* **203,** 339–342
13. Laemmli, U. K. (1970) Cleavage of structural proteins during the assembly of the head of bacteriophage T4. *Nature* **227,** 680–685
14. Schagger, H., and von Jagow, G. (1987) Tricine-sodium dodecyl sulfate-polyacrylamide gel electrophoresis for the separation of proteins in the range from 1 to 100 kDa. *Anal. Biochem.* **166,** 368–379
15. Schagger, H., and von Jagow, G. (1991) Blue native electrophoresis for isolation of membrane protein complexes in enzymatically active form. *Anal. Biochem.* **199,** 223–231
16. Bohm, G., Muhr, R., and Jaenicke, R. (1992) Quantitative analysis of protein far UV circular dichroism spectra by neural networks. *Protein Eng.* **5,** 191–195
17. De los Rios Castillo, D., Zarco-Zavala, M., Olvera-Sanchez, S., Pardo, J. P., Juarez, O., Martinez, F., Mendoza-Hernandez, G., Garcia-Trejo, J. J., and Flores-Herrera, O. (2011) Atypical cristae morphology of human syncytiotrophoblast mitochondria: role for complex V. *J. Biol. Chem.* **286,** 23911–23919
18. Lowry, O. H., Rosebrough, N. J., Farr, A. L., and Randall, R. J. (1951) Protein measurement with the Folin phenol reagent. *J. Biol. Chem.* **193,** 265–275
19. Peterson, G. L. (1977) A simplification of the protein assay method of Lowry et al. which is more generally applicable. *Anal. Biochem.* **83,** 346–356

20. Van Raaij, M. J., Orriss, G. L., Montgomery, M. G., Runswick, M. J., Fearnley, I. M., Skehel, J. M., and Walker, J. E. (1996) The ATPase inhibitor protein from bovine heart mitochondria: the minimal inhibitory sequence. *Biochemistry* **35,** 15618–15625
21. Williams, K. P., Sobral, B. W., and Dickerman, A. W. (2007) A robust species tree for the alphaproteobacteria. *J. Bacteriol.* **189,** 4578–4586
22. Gupta, R. S. (2005) Protein signatures distinctive of alpha proteobacteria and its subgroups and a model for alpha-proteobacterial evolution. *Crit. Rev. Microbiol.* **31,** 101–135
23. Zarco-Zavala, M., Morales-Rios, E., Serrano-Navarro, P., Wuthrich, K., Mendoza-Hernandez, G., Ramirez-Silva, L., and García-Trejo, J. J. (2013) Corrigendum to: The ζ subunit of the α-proteobacterial F1FO-ATP synthase in *Paracoccus denitrificans*: a novel control mechanism of the central rotor. *Biochim. Biophys. Acta Bioenergetics* **1827,** 60
24. Cabezon, E., Montgomery, M. G., Leslie, A. G., and Walker, J. E. (2003) The structure of bovine F1-ATPase in complex with its regulatory protein IF1. *Nat. Struct. Biol.* **10,** 744–750
25. Cingolani, G., and Duncan, T. M. Structure of the ATP synthase catalytic complex [F(1)] from *Escherichia coli* in an autoinhibited conformation. *Nat. Struct. Mol. Biol.* **18,** 701–707
26. Gledhill, J. R., Montgomery, M. G., Leslie, A. G., and Walker, J. E. (2007) How the regulatory protein, IF(1), inhibits F(1)-ATPase from bovine mitochondria. *Proc. Natl. Acad. Sci. U. S. A.* **104,** 15671–15676
27. Bason, J. V., Runswick, M. J., Fearnley, I. M., and Walker, J. E. Binding of the inhibitor protein IF(1) to bovine F(1)-ATPase. *J. Mol. Biol.* **406,** 443–453
28. Robinson, G. C., Bason, J. V., Montgomery, M. G., Fearnley, I. M., Mueller, D. M., Leslie, A. G., and Walker, J. E. The structure of F(1)-ATPase from *Saccharomyces cerevisiae* inhibited by its regulatory protein IF(1). *Open Biol* **3,** 120164
29. Kato, S., Yoshida, M., and Kato-Yamada, Y. (2007) Role of the epsilon subunit of thermophilic F1-ATPase as a sensor for ATP. *J. Biol. Chem.* **282,** 37618–37623
30. Schwerzmann, K., Hullihen, J., and Pedersen, P. L. (1982) Proton adenosine triphosphatase complex of rat liver mitochondria. Interaction with the ATPase inhibitor peptide covalently labeled with N-hydroxysuccinimidyl-p-azidobenzoate. *J. Biol. Chem.* **257,** 9555–9560
31. Van Heeke, G., Deforce, L., Schnizer, R. A., Shaw, R., Couton, J. M., Shaw, G., Song, P. S., and Schuster, S. M. (1993) Recombinant bovine heart mitochondrial F1-ATPase inhibitor protein: overproduction in *Escherichia coli*, purification, and structural studies. *Biochemistry* **32,** 10140–10149
32. Mizumoto, J., Kikuchi, Y., Nakanishi, Y. H., Mouri, N., Cai, A., Ohta, T., Haruyama, T., and Kato-Yamada, Y. epsilon subunit of *Bacillus subtilis* F1-ATPase relieves MgADP inhibition. *PLoS One* **8,** e73888
33. Margulis, L. (1970) *Origin of Eukaryotic Cells.* Yale University Press, New Haven, CT, USA
34. Lebowitz, M. S., and Pedersen, P. L. (1996) Protein inhibitor of mitochondrial ATP synthase: relationship of inhibitor structure to pH-dependent regulation. *Arch. Biochem. Biophys.* **330,** 342–354
35. Cabezon, E., Butler, P. J., Runswick, M. J., and Walker, J. E. (2000) Modulation of the oligomerization state of the bovine F1-ATPase inhibitor protein, IF1, by pH. *J. Biol. Chem.* **275,** 25460–25464
36. Yagi, H., Kajiwara, N., Tanaka, H., Tsukihara, T., Kato-Yamada, Y., Yoshida, M., and Akutsu, H. (2007) Structures of the thermophilic F1-ATPase epsilon subunit suggesting ATP-regulated arm motion of its C-terminal domain in F1. *Proc. Natl. Acad. Sci. U. S. A.* **104,** 11233–11238
37. Kato-Yamada, Y., and Yoshida, M. (2003) Isolated epsilon subunit of thermophilic F1-ATPase binds ATP. *J. Biol. Chem.* **278,** 36013–36016
38. Zharova, T. V., and Vinogradov, A. D. (2006) Requirement of medium ADP for the steady-state hydrolysis of ATP by the proton-translocating *Paracoccus denitrificans* Fo.F1-ATP synthase. *Biochim. Biophys. Acta* **1757,** 304–310
39. Zharova, T. V., and Vinogradov, A. D. (2004) Energy-dependent transformation of F0.F1-ATPase in Paracoccus denitrificans plasma membranes. *J. Biol. Chem.* **279,** 12319–12324
40. Perez, J. A., and Ferguson, S. J. (1990) Kinetics of oxidative phosphorylation in *Paracoccus denitrificans*. 1. Mechanism of ATP synthesis at the active site(s) of F0F1-ATPase. *Biochemistry* **29,** 10503–10518
41. Perez, J. A., and Ferguson, S. J. (1990) Kinetics of oxidative phosphorylation in *Paracoccus denitrificans*. 2. Evidence for a kinetic and thermodynamic modulation of F0F1-ATPase by the activity of the respiratory chain. *Biochemistry* **29,** 10518–10526

Received for publication September 4, 2013.
Accepted for publication January 27, 2014.